Photoinduced Phase Transition to a New Macroscopic Spin-Crossover-Complex Phase

Takeshi Tayagaki and Koichiro Tanaka
Department of Physics, Graduate School of Science, Kyoto University, Kyoto 606-8502, Japan

(Received 13 December 2000)

We clarified for the first time that the photoinduced phase is quite different in structure from the thermally induced phase by the resonant Raman spectroscopy in the spin-crossover complex, $[\mathrm{Fe(2\text{-}pic)_3}]\mathrm{Cl_2EtOH}$. In the photoinduced phase we observed a number of additional lines assigned to infra-active vibrational modes which are strongly prohibited by selection rules in the thermally induced phase. These results indicate that a dramatic symmetry lowering should take place in the photoinduced phase. The cooperative Jahn-Teller transformation is a plausible candidate for the symmetry lowering in the photoinduced phase.

DOI: 10.1103/PhysRevLett.86.2886 PACS numbers: 78.90.+t, 64.90.+b, 78.30.−j

In recent years, photoinduced cooperative transition phenomena have been widely studied in several materials [1–4]. These phenomena include common nonlinear characteristics such as the existence of the threshold light intensity and the incubation period, suggesting that cooperative interaction plays an important role in the photoexcited state. From this point, such phenomena are called "photoinduced phase transition" [5]. Photoinduced phase transition is closely related to multistability of the ground state in the material: Light irradiation stimulates the macroscopic phase transition between the *true* ground state and the metastable state, although thermal fluctuation triggers the thermal phase transition. It has been believed that the photoinduced phase is the same state as the thermally induced phase, because the absorption spectra, magnetic property [1], and reflection spectra [2,3] in the photoinduced phase are similar to those in the thermally induced phase.

In this Letter, we investigate the photoinduced phase transition in the spin-crossover complex by the resonant Raman scattering and clarify experimentally that the photoinduced phase is a new macroscopic phase which has quite different structure from the thermally induced phase.

Spin-crossover complexes have been studied extensively as attractive materials, whose magnetic and chromatic properties can be controlled with external stimuli such as heat, pressure, magnetic field, and so on [6]. In this study, single crystals of $[\mathrm{Fe(2\text{-}pic)_3}]\mathrm{Cl_2EtOH}$ are prepared by the evaporation method. The Fe^{2+} ion is octahedrally surrounded by six nitrogen atoms in three 2-picolylamine molecules. The unit cell is composed of four octahedral $[\mathrm{FeN_6}]^{2+}$ clusters [7]. The d^6 electrons of the Fe^{2+} ion which feels an approximate cubic ligand field may take two different states due to competition between Coulomb repulsion among the electrons and ligand-field splitting between t_{2g} and e_g orbitals: In the weak ligand field, the ground state takes a high-spin state $S = 2$, while in the strong field, it takes a low-spin state $S = 0$. From the magnetic susceptibility measurement by SQUID from 4.2 to 300 K, $[\mathrm{Fe(2\text{-}pic)_3}]\mathrm{Cl_2EtOH}$ has a paramagnetic phase ($^5T_2$) at room temperature. With lowering temperature, a first-order phase transition takes place from the paramagnetic phase to the diamagnetic phase ($^1A_1$) in two steps at critical temperatures of 114 and 122 K [6,8]. Figure 1 shows absorption spectra at 100 and 300 K. One can find a dramatic spectral change by the spin-crossover transition. Absorption band at 1.5 eV (2.0 eV) corresponds to the transition from $^5T_2$ ($^1A_1$) to ^5E ($^1T_1$) in the paramagnetic (diamagnetic) phase, where the sample color is yellow (red). Insets show electron configurations of the ground states in these phases. The spin-crossover transition can also be induced by light irradiation, which is called "light induced excited spin state trapping" (LIESST) [6,9]. In $[\mathrm{Fe(2\text{-}pic)_3}]\mathrm{Cl_2EtOH}$, light irradiation below 40 K leads to LIESST, where the sample color changes from red to yellow [10]. Recently, Ogawa *et al.* reported that LIESST in $[\mathrm{Fe(2\text{-}pic)_3}]\mathrm{Cl_2EtOH}$ shows nonlinear characteristics such as thresholdlike behavior, incubation period, and phase separation [1]. They attributed the photoinduced phase to be the same state as the thermally induced

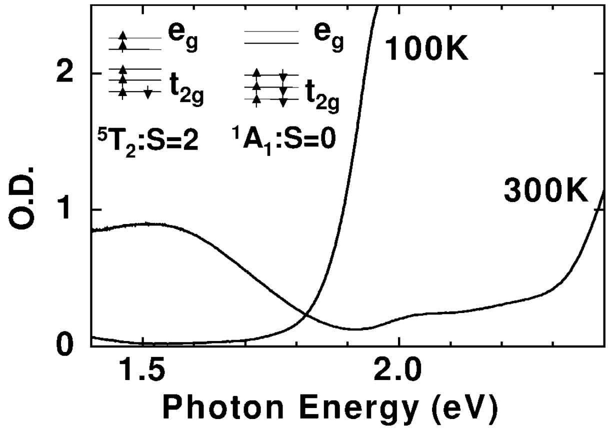

FIG. 1. Absorption spectra in the $[\mathrm{Fe(2\text{-}pic)_3}]\mathrm{Cl_2EtOH}$ single crystal measured at 300 and 100 K. Absorption band at 1.5 eV (2.0 eV) corresponds to the *d*-*d* transition in the paramagnetic (diamagnetic) phase. The insets show electron configurations of the ground state in these phases.

paramagnetic phase because the absorption spectrum and magnetic property in the photoinduced phase are quite similar to those in the high-temperature phase.

Figure 2 shows Raman spectra of $[Fe(2\text{-pic})_3]Cl_2EtOH$ single crystal measured at (a) 300, (b) 70, and (c) 30 K, corresponding to (a) high-temperature phase, (b) low-temperature phase, and (c) photoinduced phase, respectively. We used the second harmonics of cw-neodymium vanadate (Nd:YVO_4) laser (2.33 eV) as the excitation light source. The scattered light was collected in the $z(xx)\bar{z}$ configuration and dispersed by a triple polychromater. Raman signals were detected by a liquid-nitrogen-cooled charge-coupled-device detector. We also used Ar^+ laser (488 nm) and observed the similar Raman spectra, which means that the spectrum is not a fluorescence but Raman scattering light. Below 40 K, photoinduced phase transition simultaneously takes place with irradiation of the laser by which Raman spectra are measured. We confirmed the chromatic change from red to yellow by laser irradiation, as reported in Refs. [1] and [10].

As shown in Figs. 2(a) and 2(b), Raman spectra in the high- and the low-temperature phase have quite similar structures except for relative signal intensities. We assigned lines indicated by $p1-p5$ in Fig. 2(a) to vibrational modes of the picolylamine molecule by referring the Raman spectrum of the 2-picolylamine molecule. The peaks A and B should be related to the vibrational mode of the $[FeN_6]^{2+}$ cluster. The difference in the intensity between two phases can be understood by the resonant enhancement of the Raman efficiency: The lines $p1-p5$ are stronger (weaker) than A and B in the high (low) temperature phase. The exciting 2.33 eV light is resonant to the $t_{2g} \rightarrow e_g$ transition of Fe^{2+} ion in the low-temperature phase, whereas it is resonant to the picolylamine molecular in the high-temperature phase.

In the photoinduced phase a number of additional lines appear below 750 cm^{-1} which are not observed in the high- and low-temperature phases. These features disappear quickly when temperature is raised above 40 K and are never seen in the Raman spectrum measured with the laser light that cannot induce the phase transition (e.g., 1.5 eV). This indicates that a photoinduced change in the Raman spectrum should be an intrinsic and reproducible process. The appearance of Raman lines strongly suggests that a symmetry lowering should take place in the photoinduced phase. From the intensities of lines $p2-p5$, the photoinduced phase seems to be close to the high-temperature phase.

Figure 3(b) shows the infrared absorption spectrum measured at 300 K. The powder sample was diluted with KBr and compressed to form a pellet. Additional Raman lines in the photoinduced phase shown by C, D, and E are clearly attributed to infrared lines which are assigned to the vibrations of the picolylamine molecule in the high-temperature phase. Table I summarizes peaks and relative intensities of lines in the Raman spectrum and in the infrared spectrum. Lines indicated by D and E in the Raman spectrum shift to the lower frequency side from those in the infrared spectrum, although line C is almost unchanged. The shifts in D and E suggest that mode softening should take place in the photoinduced phase by structural distortion of the picolylamine molecule. The relative intensities

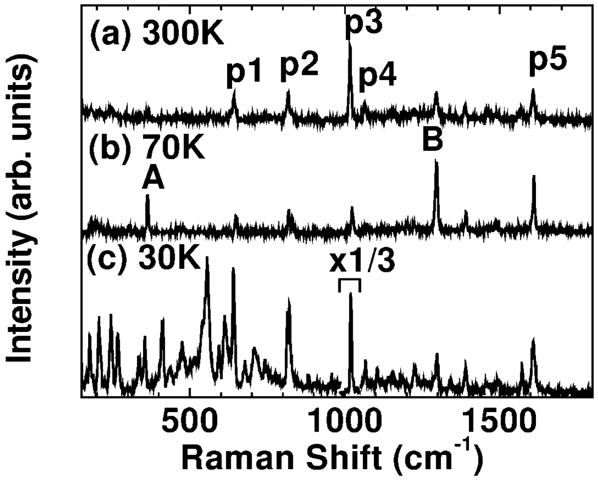

FIG. 2. Raman spectra of the $[Fe(2\text{-pic})_3]Cl_2EtOH$ single crystal measured at (a) 300 K, (b) 70 K, and (c) 30 K. The light source is the second harmonic of cw-Nd:YVO_4 laser, 2.33 eV. The labels $p1-p5$ show vibrations of the 2-picolylamine molecules. Labels A and B are described in the text.

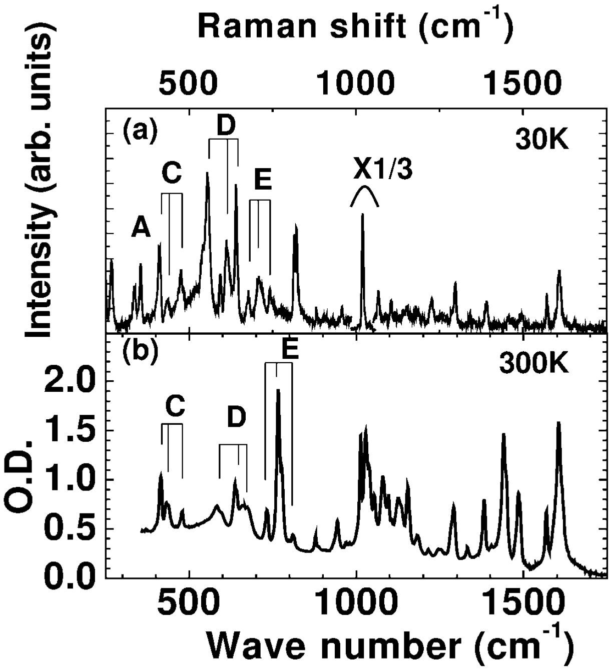

FIG. 3. (a) Raman spectrum measured in the photoinduced phase. (b) Infrared absorption spectrum of the $[Fe(2\text{-pic})_3]$-Cl_2EtOH powder measured at 300 K. Labels C–E are described in the text.

TABLE I. Peaks and relative intensities of lines in the Raman spectrum (photoinduced phase) and in the infrared absorption spectrum (high-temperature phase). Intensities are normalized by the largest peak.

Peak	Peak position (cm^{-1}) Raman	Peak position (cm^{-1}) Infrared	Peak shift (cm^{-1})	Relative intensity Raman	Relative intensity Infrared
$C(1)$	411	416	5	0.53	0.54
$C(2)$	438	437	−1	0.22	0.39
$C(3)$	476	479	3	0.39	0.35
$D(1)$	555	583	28	1	0.38
$D(2)$	612	637	25	0.58	0.50
$D(3)$	640	667	27	0.92	0.38
$E(1)$	678	733	55	0.27	0.36
$E(2)$	707	767	60	0.33	1
$E(3)$	741	810	69	0.27	0.23

of the additional Raman lines in the photoinduced phase and the infrared lines behave complementary: In the Raman spectrum $E \leq C \leq D$, while in the infrared spectrum $D \leq C \leq E$. These results suggest infra-active modes of the picolylamine molecule should strongly couple with the electronic state in the photoinduced phase.

The breathing mode (totally symmetric mode) of the $[\mathrm{FeN}_6]^{2+}$ cluster has accounted so far for the photoinduced phase transition from diamagnetic to paramagnetic, which also contributes to the cooperative elastic interaction [1,11]. However, this mechanism cannot explain the symmetry lowering characteristics observed in the Raman spectrum. To explain the obtained results, we make a theoretical consideration on the assumption that the photoinduced phase is stabilized by the cooperative Jahn-Teller transformation. For simplicity, our model includes only d^6 electrons in the $[\mathrm{FeN}_6]^{2+}$ cluster with 2 order parameters: breathing mode (A_{1g}) and Jahn-Teller mode (E_g or T_{2g}). Figure 4(a) shows the schematic free energy diagram of this model. At 0 K, *true* ground state is the diamagnetic phase (F_{dia}). The paramagnetic phase ($^5T_2$) should be unstable since the paramagnetic state has threefold orbital degeneracy. This leads to the Jahn-Teller effect and transforms $^5T_2$ to the lower symmetric state. The Jahn-Teller effect plays cooperatively among clusters to induce a new ordered phase (F_{JT}). As a result, the free energies of three phases satisfy

$$F_{\mathrm{dia}} < F_{\mathrm{JT}} < F_{\mathrm{para}} \,. \tag{1}$$

The Jahn-Teller phase should be a metastable phase. At finite temperatures, the entropy S plays an important role in free energy, as shown in Eq (2):

$$F = E - ST \,. \tag{2}$$

Because of orbital triplet and spin quintet, the paramagnetic phase ($^5T_2$) has 15-fold degeneracy [6]. In the cooperative Jahn-Teller phase, spin degeneracy is left while orbital degeneracy is dissolved. The entropy is therefore calculated as follows:

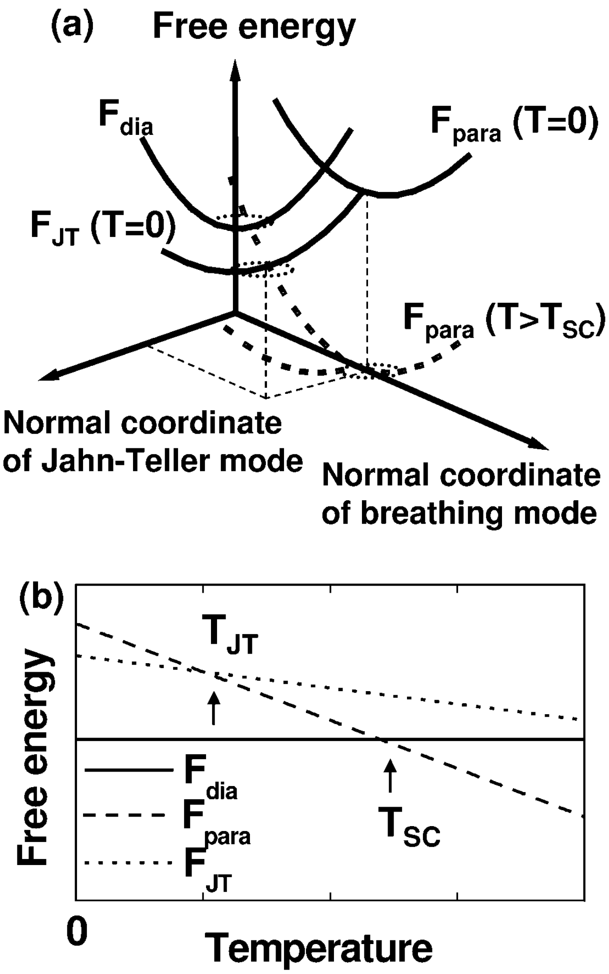

FIG. 4. (a) Schematic free energy diagram of the model including d^6 electrons in $[\mathrm{FeN}_6]^{2+}$ cluster with 2 order parameters: breathing mode (A_{1g}) and Jahn-Teller mode (E_g or T_{2g}). Solid lines show the free energy diagram at 0 K. Dashed lines show the free energy at high temperatures ($T > T_{\mathrm{SC}}$). F_{dia}, F_{para}, and F_{JT} represent the free energy of the diamagnetic, paramagnetic, and Jahn-Teller phase, respectively. (b) Temperature dependence of the free energy in the diamagnetic phase, paramagnetic phase, and the Jahn-Teller phase on the assumption of Eqs. (2) and (3). $T_{\mathrm{SC(JT)}}$ shows the critical temperature of the spin-crossover transition (cooperative Jahn-Teller transformation). In the calculation, we set free energies at 0 K to satisfy $T_{\mathrm{JT}} < T_{\mathrm{SC}}$.

$$S_{\mathrm{dia}} = 0 \,, \tag{3a}$$

$$S_{\mathrm{para}} = k_B \log 15 \,, \tag{3b}$$

$$S_{\mathrm{JT}} = k_B \log 5 \,. \tag{3c}$$

Figure 4(b) shows calculations of free energies under conditions of Eqs. (2) and (3). At the high temperature limit, the entropy governs phase stability. The free energies of three phases become

$$F_{\mathrm{para}} < F_{\mathrm{JT}} < F_{\mathrm{dia}} \,. \tag{4}$$

In this model, thermal phase transition therefore takes place at T_{SC} as shown in Fig. 4(b). Photoinduced phase transition can be considered as the macroscopic transition from the diamagnetic phase not to the paramagnetic phase but to the Jahn-Teller phase below T_{TJ}. From the point of the dynamical process, the photoexcited state ($^1T_1$ or $^1T_2$) in the diamagnetic phase may also induce the Jahn-Teller effect because of orbital degeneracy. This should trigger the photoinduced phase transition. Based on this mechanism, appearances of Raman lines in the photoinduced phase can be understood as follows: The Jahn-Teller distortion of the $[FeN_6]^{2+}$ cluster leads to the stretching of the picolylamine molecule, where picolylamine molecules distort differently from those in the thermally induced phase. These structural changes make the coupling between electrons and infra-active modes stronger only in the soft vibrational region related to stretching distortion of the molecule. As a result, infra-active modes appear additionally in the Raman spectrum in the photoinduced phase.

In conclusion, we observed that the Raman spectrum in the photoinduced phase appears quite differently from those in the thermally induced phase. The spectral change strongly indicates that symmetry lowering takes place in the photoinduced phase. The spectral change of Raman scattering can be understood qualitatively on the assumption of the cooperative Jahn-Teller transformation in the photoinduced phase. This is the first observation of the difference between the photoinduced phase and the thermally induced phase. In other words, the photoinduced phase transition can realize a new material ordering that is hidden in the thermal phase transition. The cooperative Jahn-Teller transformation is a strong candidate to contribute to the photoinduced phase transition as a long-range interaction. In order to confirm the Jahn-Teller effect in the photoinduced phase, the local structure should be clarified by ESR or EXAFS measurements.

The authors thank Professor S. Koshihara and Mr. Y. Ogawa for teaching the crystal-growth method and Mr. M. Shirai and Mr. N. Yonemura for their kind help in experiments. The authors are grateful to Professor K. Nasu and Professor K. Kan'no for fruitful discussions, and to Professor K. Tamimura for support in Raman scattering measurements. This work is partially supported by a Grant-in-Aid for Scientific Research on Priority Areas, "Photo-induced Phase Transition and Their Dynamics," from the Ministry of Education, Science, Sports and Culture of Japan.

[1] Y. Ogawa, S. Koshihara, K. Koshino, T. Ogawa, C. Urano, and H. Takagi, Phys. Rev. Lett. **84**, 3181 (2000).
[2] S. Koshihara, Y. Tokura, K. Takeda, and T. Koda, Phys. Rev. Lett. **68**, 1148 (1992).
[3] S. Koshihara, Y. Tokura, T. Mitani, G. Saito, and T. Koda, Phys. Rev. B **42**, 6853 (1990).
[4] K. Miyano, T. Tanaka, Y. Tomioka, and Y. Tokura, Phys. Rev. Lett. **78**, 4257 (1997).
[5] *Relaxation of Excited States and Photo-Induced Structural Phase Transitions,* edited by K. Nasu (Springer-Verlag, Berlin, 1997).
[6] P. Gütlich, A. Hauser, and H. Spiering, Angew. Chem. **33**, 2024 (1994).
[7] M. Mikami, M. Konno, and Y. Saito, Acta Cryst. **36**, 275 (1980).
[8] M. Sorai, J. Ensling, and P. Gütlich, Chem. Phys. **18**, 199 (1976).
[9] A. Hauser, J. Chem. Phys. **94**, 2741 (1991).
[10] S. Decurtins, P. Gütlich, K. M. Hasselbach, A. Hauser, and H. Spiering, Inorg. Chem. **24**, 2174 (1985).
[11] K. Koshino and T. Ogawa, J. Phys. Soc. Jpn. **68**, 2164 (1999).